

Heterogeneous & Homogeneous & Bio- & Nano-

CHEM **CAT** CHEM

CATALYSIS

Accepted Article

Title: Single-Site Molybdenum Catalyst for the Synthesis of Fumarate

Authors: Huifang Jiang, Rui Lu, Xiaoqin Si, Xiaolin Luo, Jie Xu, and Fang Lu

This manuscript has been accepted after peer review and appears as an Accepted Article online prior to editing, proofing, and formal publication of the final Version of Record (VoR). This work is currently citable by using the Digital Object Identifier (DOI) given below. The VoR will be published online in Early View as soon as possible and may be different to this Accepted Article as a result of editing. Readers should obtain the VoR from the journal website shown below when it is published to ensure accuracy of information. The authors are responsible for the content of this Accepted Article.

To be cited as: *ChemCatChem* 10.1002/cctc.201900332

Link to VoR: <http://dx.doi.org/10.1002/cctc.201900332>

WILEY-VCH

www.chemcatchem.org



COMMUNICATION

Single-Site Molybdenum Catalyst for the Synthesis of Fumarate

Huifang Jiang,^{[a],[b]} Rui Lu,^[a] Xiaoqin Si,^{[a],[b]} Xiaolin Luo,^{[a],[b]} Jie Xu,^[a] and Fang Lu^{*[a]}

Dedicated to the 70th anniversary of Dalian Institute of Chemical Physics, CAS

Abstract: The catalysts with well-defined mononuclear active sites are expected to develop more active catalytic systems for the key chemical transformations. But the rational design of catalyst with stable mononuclear Mo site is still a crucial challenge because of its oligomerization tendency under reaction condition. Herein, Molybdenum catalyst (Mo-8-HQ) with single Mo sites was designed via the pyridine nitrogen and oxygen in hydroxyl of 8-hydroxyquinoline coordinated with Mo atom. The crystal catalyst was stabilized by π - π stacking interaction and hydrogen bonds to form isolated Mo specie. The single-site molybdenum catalyst exhibited excellent catalytic performance in didehydroxylation reactions with highly selective of dibutyl fumarate (86%) product at mild reaction condition. Deuterium isotopic studies demonstrated that the mechanism feature of didehydroxylation reaction catalyzed by Mo-8-HQ was through concerted cleavage of two C-O bonds process, which could be accelerated by single-site molybdenum catalysts with electron-rich Mo centers.

Renewable and abundant biomass resources as one of the most promising feedstocks have received tremendous interests in both academia and industry.^[1] In contrast with fossil resources, the basic units of cellulose and hemicellulose in biomass contain polyhydroxy structures resulting in high oxygen to carbon ratio.^[2] Especially, sugar acid, which contains terminal carboxylic functionalities and polyhydroxy groups, could be the most promising candidate for synthesizing commonly used dicarboxylic acid monomers of polymers industry, such as fumaric acid, succinic acid and adipic acid.^[3] The key challenge of this sustainable route is to develop high-effective catalytic systems which can selectively remove oxygens in the bioresource. Among various deoxygenation reactions, for instance high-temperature pyrolysis^[4], hydrodeoxygenation^[5], hydrogenolysis reactions^[6] and acid-catalyzed dehydration^[7], the didehydroxylation reactions can efficiently remove two adjacent hydroxyl groups of polyols in one-step by converting vicinal diols into alkenes.^[8]

Molybdenum based catalysts are the best and versatile catalysts of many industrially important reactions, such as polymerization reactions^[9], olefin epoxidation^[10] and olefin metathesis^[11]. Recently, inorganic Mo-based catalysts and a few of organic Mo complex catalysts have been explored to catalyze

didehydroxylation reactions of polyols.^[12] While most Mo species exhibit moderate performance to form olefin products, and high temperature in the range of 200-250 °C was normally required.^[13] Polynuclearity in the original Mo structure and aggregation of Mo catalysts at reaction condition might be the main reasons for the low activity.^[14] Therefore, substantial challenges remain towards the goal of establishing a new strategy for the synthesis of stable single-site Mo catalysts.

In this work, 8-quinolinol molybdenum complex (Mo-8-HQ) catalyst with single Mo sites was synthesized. The pyridine nitrogen and oxygen in hydroxyl of 8-hydroxyquinoline coordinated with Mo atom to form isolated Mo specie. The crystal catalyst was stabilized by π - π stacking interaction and hydrogen bonds. Tartaric acid (TA) and tartrate with adjacent hydroxyls as the sugar acid derivatives, which can be catalytically converted into the important building block chemicals, were chosen as the substrates to study the didehydroxylation reaction mechanism in view of its simple chain structure feature. Under mild reaction conditions, the mononuclear Mo-8-HQ catalyst exhibited excellent catalytic performance in didehydroxylation reactions with a highly selective dibutyl fumarate (86%) product via the concerted pathway.

MoO₂(acac)₂ and 8-hydroxyquinoline (8-HQ) ligand were used as the starting materials to prepare the 8-quinolinol molybdenum complex (Mo-8-HQ) by the ligand exchange method. The experimental detail is explained in Supporting Information. Through comparing the FTIR spectroscopy (Figure 1a) of Mo-8-HQ with 8-hydroxyquinoline and MoO₂(acac)₂, the presence of two infrared bands at the 894 and 942 cm⁻¹ attributed to $\nu_{as}(\text{O}=\text{Mo}=\text{O})$ and $\nu_s(\text{O}=\text{Mo}=\text{O})$ in C_{2v} symmetry, respectively, indicated the *cis* conformation of the MoO₂ (*cis*-MoO₂) moiety.^[15] The infrared broad band centered around 3115 cm⁻¹ in 8-HQ belong to $\nu(\text{O}-\text{H})$. This broad band disappeared in Mo-8-HQ catalyst due to the hydroxyl group in 8-hydroxyquinoline ligand coordinating with molybdenum atom. This was also confirmed by the new band appeared at 537 cm⁻¹ in Mo-8-HQ, which could be assigned to $\nu(\text{Mo}-\text{O})$. The presence of the band at 497 cm⁻¹ was assigned to $\nu(\text{Mo}-\text{N})$ vibration model in Mo-8-HQ. In view of these characters, we speculated the structure of Mo-8-HQ is 8-HQ molecules coordinating with Mo atom through pyridine nitrogen and oxygen in hydroxyl.

The crystalline nature of the prepared Mo-8-HQ was characterized by powder X-ray diffraction (XRD). The powder XRD pattern (Figure 1b) showed that Mo-8-HQ had a new structure with good crystallinity compared with 8-HQ and MoO₂(acac)₂. And its main diffraction peaks could match with bis(molybdenum bis(8-quinolinol)) oxide (JPCDS No. 26-1950), which means our Mo-8-HQ catalyst is analogous with bis(molybdenum bis(8-quinolinol)) oxide, in other words, one *cis*-MoO₂ moiety probably combined with two 8-HQ molecules to form one 8-quinolinol molybdenum unit.

The valence of molybdenum and the effect of N ligand in Mo-8-HQ were investigated by X-ray photoelectron spectroscopy

[a] H. Jiang, R. Lu, X. Si, X. Luo, Prof. Dr. J. Xu, Prof. Dr. F. Lu
State Key Laboratory of Catalysis, Dalian Institute of Chemical Physics, Chinese Academy of Sciences, Dalian National Laboratory for Clean Energy, 457 Zhongshan Road, Dalian 116023 (P.R. China)
E-mail: lufang@dicp.ac.cn

[b] H. Jiang, X. Si, X. Luo
University of Chinese Academy of Sciences
Beijing 100049 (P.R. China)

Supporting information for this article is available on the WWW under <http://doi.org/10.1002/cctc.201900332>

COMMUNICATION

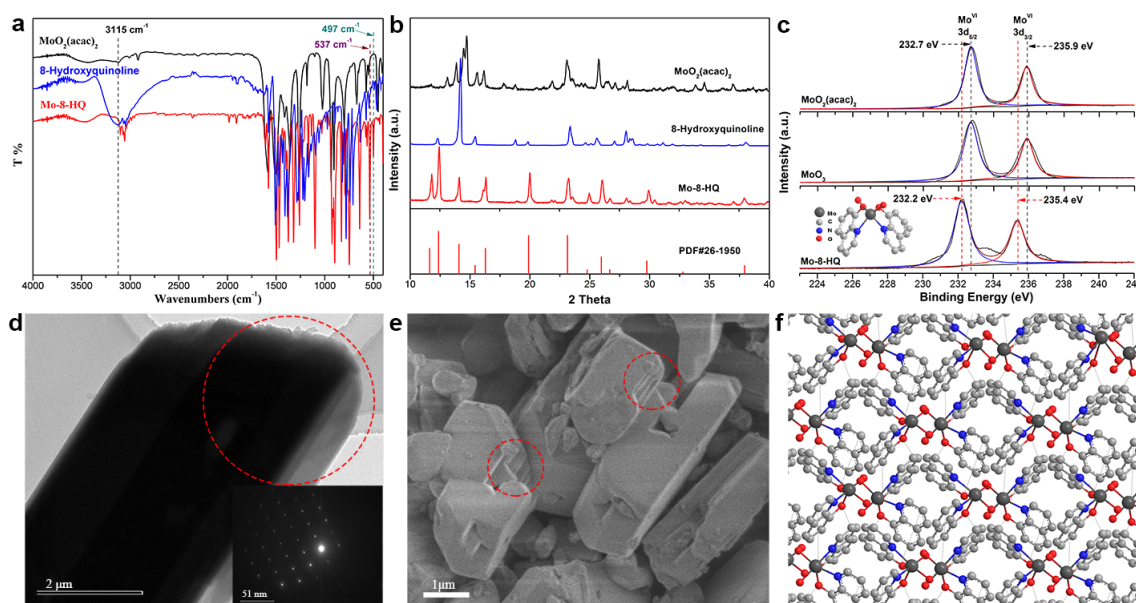


Figure 1. (a) FTIR spectroscopy of $\text{MoO}_2(\text{acac})_2$, 8-hydroxyquinoline and Mo-8-HQ. (b) XRD of $\text{MoO}_2(\text{acac})_2$, 8-hydroxyquinoline and Mo-8-HQ. (c) XPS spectra of $\text{MoO}_2(\text{acac})_2$, MoO_3 and Mo-8-HQ, proposed construction unit of Mo-8-HQ was inset of (c). (d) SAED pattern of Mo-8-HQ. (e) SEM image of Mo-8-HQ. (f) Proposed stacking structure of Mo-8-HQ. Molybdenum, oxygen, carbon and nitrogen atoms are black, red, gray and blue, respectively.

(XPS). In the Mo 3d XPS spectra (Figure 1c), two distinct peaks of $\text{Mo}^{\text{VI}} 3d_{5/2}$ and $\text{Mo}^{\text{VI}} 3d_{3/2}$ appeared at binding energies of 232.2 and 235.4 eV, respectively, which were closed to, but lower by ca. 0.5 eV than that of Mo^{VI} in MoO_3 and $\text{MoO}_2(\text{acac})_2$ (232.7 and 235.9 eV).^[16] The peak shifted of $\text{Mo}^{\text{VI}} 3d_{5/2}$ and $3d_{3/2}$ might be attributed to the pyridine nitrogen coordination with Mo, which leads to the electron donating effect from nitrogen to Mo atom and situates Mo atom in a rich electron condition. Aforementioned, we deduced from FTIR and XRD, one Mo^{VI} in *cis*- MoO_2 moiety probably coordinated with two 8-HQ ligands via pyridine nitrogen and oxygen in hydroxyl and assembled into Mo-8-HQ molecule, i.e. $\text{MoO}_2(\text{oxine})_2$. Its construction unit was shown as the inset of Figure 1c.

The selected-area electron diffraction (SAED) pattern of the bulk Mo-8-HQ particles was shown in Figure 1d. It exhibited regular diffraction spots, which indicated that Mo-8-HQ posed single crystal feature. The SEM image showed Mo-8-HQ particles presented a prism shape and every prism was stacked via several layers (Figure 1e). The EDS analysis (see the Supporting Information, Figure S1) revealed that Mo-8-HQ consisted of Mo, C, N and O, which was also proved by element distribution maps (Figure S2).

Therefore, the proposed construction structure of Mo-8-HQ contained one with Mo^{VI} as the single active sites,^[17] and after coordinated with two 8-HQ ligands, it will become a more stable organic Mo complex. According to the reported analogues,^[18] each construction unit of Mo-8-HQ was likely to assemble through π - π stacking interaction to form layers and through hydrogen bonds between layers to build up the prism single crystal structures as shown in Figure 1f.

Various commercially available Mo compounds with different valence states, such as Mo powder (0), $\text{Mo}_2(\text{CH}_3\text{COO})_4$ (II), MoO_2 (IV), MoS_2 (IV), MoCl_5 (V), H_2MoO_4 (VI), MoO_3 (VI), $(\text{NH}_4)_6\text{Mo}_7\text{O}_{24}$ (VI) and $\text{MoO}_2(\text{acac})_2$ (VI) were investigated in the

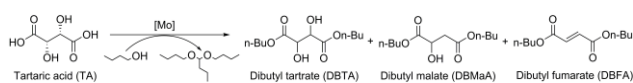
didehydroxylation of tartaric acid. The catalytic activities of these molybdenum catalysts were examined in glovebox filled with argon to keep the Mo catalysts stable before reactions. Then the didehydroxylation reactions were typically performed at 160 °C over a period of 12 h and biomass-derived 1-butanol was used as the solvent and reductant.

After the reaction, dibutyl tartrate (DBTA), dibutyl malate (DBMaA), dibutyl fumarate (DBFA) and acetal were detected (Scheme 1). DBTA was the esterification product of tartaric acid and 1-butanol. And 1-butanol as the main oxidized product, which was generated directly from the hydrogen transfer process of 1-butanol and trapped as acetal, which has been determined by GC-MS. The acetal increased following dibutyl fumarate product as reaction time was prolonged (as shown in Figure S3).

All the results were summarized in Figure 2a, the total yield of deoxygenate products DBFA and DBMaA varies greatly with the different valence states of molybdenum. Even though most Mo compounds were active, it was obvious that molybdenum catalysts with VI state had a better catalytic efficiency. However, the normal Mo^{VI} , for instance, MoO_3 and H_2MoO_4 , were showed lower product yield. This different behaviour could probably due to the low solubility of these bulk solid catalysts during the reaction process. When using $\text{MoO}_2(\text{acac})_2$ as the catalyst, the combined yield of deoxygenated species increased to 37%, but it still had great potential to improve. We designed a type of Mo-8-HQ catalyst with single molybdenum sites, interestingly, it showed the highest DBFA yield (ca. 74%, as shown in Figure 2a), a significant increase compared to other Mo-based catalysts. We further employed the preparation procedure at air condition, and similar products yield could be obtained. It means that the harsh reaction condition without oxygen and water was not the essential element for our catalyst. When DBTA was used as the starting material for this didehydroxylation reaction (Scheme S1 and Figure S4), the reaction proceeded only slightly faster than that of TA, and DBTA

COMMUNICATION

could be converted into DBFA with the highest yield of 86%. This result suggested that TA was first inclined to esterification before undergoing the didehydroxylation process.



Scheme 1. Didehydroxylation reaction of tartaric acid using [Mo] catalysts in 1-butanol.

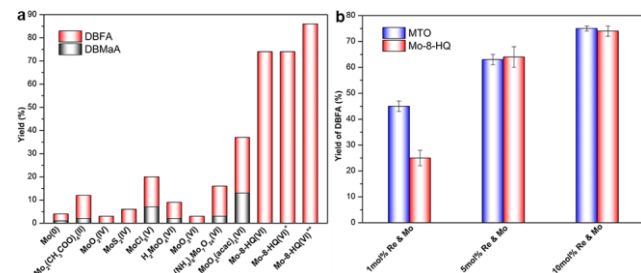


Figure 2. (a) Didehydroxylation reactions of the tartaric acid with different Mo catalysts. Reaction conditions: 0.25 mmol L-tartaric acid, 10 mol% Mo catalyst and 5 mL 1-butanol were added into 38 mL glass vessel, which was operated in glovebox, then wrapped by Al foil, put into oil bath and kept at 160 °C for 12 h. “*” means preparing procedure was operated in air condition. “***” means DBTA was used as the starting material. (b) Didehydroxylation reactions of the tartaric acid with different mole ratios of methyltrioxorhenium (MTO) and Mo-8-HQ catalysts at 160 °C for 12 h in air.

Rhenium (Re)-based catalyst has been reported as the most effective catalyst for the didehydroxylation reaction due to its special oxophilic ability and multiple oxidation states.^[19] However, the intrinsic properties of Re hampered the implementation of the didehydroxylation process on boosting industrial scale, as it is a remarkably scarce element and easy to sublime in preparing process. Figure 2b showed the catalytic performance comparison between Re and Mo-8-HQ catalysts with adding different molar ratios. Obviously, the amount of catalysts had an effect on the reaction. Although Mo-8-HQ showed a lower DBFA yield at 1 mol%, it had a similar DBFA yield when the catalyst amount more than 5 mol%. We thus envisioned that the Mo-8-HQ has the great potential to replace Re catalyst.

It has been reported that the reduction of the high-valent metal oxide center and extrusion of the alkene were the rate-limiting transition state by DFT calculation for the didehydroxylation of diol.^[13b] Aforementioned, the nitrogen as an electron donor in 8-HQ ligand compelled Mo atom in the rich electron condition. Thus, it is possible that Mo atom in Mo-8-HQ will easily lose electrons during its redox process, which is vital for conquering the rate-limiting transition procedure. In addition, the literature shows that only strong ligand can form stable Mo catalyst.^[13c] 8-HQ is a ligand with good coordinating capacities, coordinated with Mo atom through pyridine nitrogen and oxygen in hydroxyl. Compared with Mo-8-HQ catalyst, MoO₂(acac)₂ has very loosely bound ligands, and its coordinating structure will be destroyed easily during the reaction process, resulting in deactivation. Moreover, Mo-8-HQ catalyst with single Mo sites was further stabilized through π - π stacking interaction and hydrogen bonds in ligand. Therefore, we hold the view that the excellent catalytic performance of Mo-8-HQ might be attributed to stable single Mo sites and rich electron condition of Mo centers.

Kinetic studies exhibited that tartaric acid was gradually converted into DBFA product with C=C bond in 160 °C, as shown in Figure 3a. The yield of dibutyl fumarate and dibutyl malate increased continuously with MoO₂(acac)₂ catalyst. Meanwhile, there was no dibutyl malate as byproduct with Mo-8-HQ catalyst, and this was similar to methyltrioxorhenium catalyst (MTO) (Figure S5). It was also confirmed via real-time in situ FTIR, the didehydroxylation of dibutyl tartrate was monitored real time by in situ FTIR spectroscopy. The peaks at 1300 cm⁻¹ corresponded to the C-O stretching vibrations of DBFA^[20] (Figure 3b and Figure S6), respectively. It elucidated that DBFA was produced and accumulated gradually. In addition, except for DBFA, no other products were observed by real-time in situ FTIR spectroscopy, consistent with the high selectivity observed by the GC-MS (the typical total ion chromatogram (TIC) spectrum was shown in Figure S7).

After completion of didehydroxylation reaction, a yellow powder was separated out from the reaction products by filtration, then washed with 1-butanol and dried by vacuum. The separated catalyst was put into a new didehydroxylation reaction of tartaric acid (TA). The yield of dibutyl fumarate (DBFA) was ca. 52%, lower than the first run (ca.74%). As shown in Figure S8, the infrared spectrum of used catalyst could match well with fresh Mo-8-HQ, except some 1-butanol peaks appears (1-butanol cannot be removed totally). Thus, it is viable that Mo-8-HQ can be separated without changing its structure after reaction. So, the reason of lower DBFA yield with separated catalyst was possibly that a part of the catalyst dissolved in the solvent after reaction and cannot be totally separated (the initial catalyst input was ca. 10 mg, and only ca. 0.7 mg was separated). We added a little fresh Mo-8-HQ into the separated catalyst to make the mass up to 10 mg, then the yield of dibutyl fumarate (DBFA) was ca. 70% in a new didehydroxylation reaction.

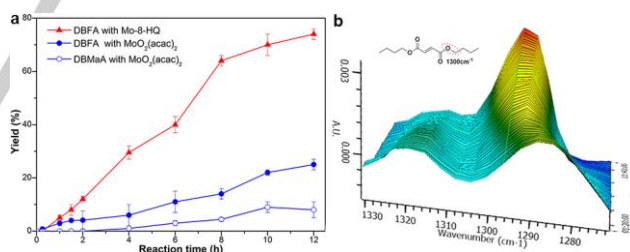


Figure 3. (a) Didehydroxylation reaction of tartaric acid catalyzed by Mo-8-HQ (10 mol% Mo) and MoO₂(acac)₂ (10 mol% Mo) at 160 °C, respectively. (b) Real-time in situ FTIR spectroscopic analysis of the didehydroxylation reaction of DBTA in 1-butanol. The peaks at 1300 cm⁻¹ corresponded to the C-O stretching vibrations of DBFA. Reaction conditions: DBTA (2 mmol), Mo-8-HQ (10 mol%), 1-butanol (10 mL), 155 °C.

According to our experiments, except the main product DBFA, DBMaA was a kind of side product with MoO₂(acac)₂ as the catalyst. While using Mo-8-HQ catalyst, the reaction was highly selective with DBFA as the unique product and no other byproduct was observed. As reported before,^[13b, 14c, 21] there were two possible pathways of didehydroxylation for tartaric acid (as shown in Figure 4a). Path 1 is the concerted pathway via breaking two C-O bonds, and path 2 is the stepwise pathway via a sequential “dehydration–reduction–dehydration” procedure. Because of the reduced steric effect of the primary 1-butanol, the esterification

COMMUNICATION

step of tartaric acid can be finished quickly.^[8c] Herein, we hypothesize the esterification step cannot influence the mechanism of didehydroxylation process. Path 1 (shown in Figure 4a with red dot line), adjacent hydroxyls in tartaric acid can be removed by concerted cleavage of two C-O bonds and generated DBFA. Path 2 (shown in Figure 4a with blue dot line), at first, tartaric acid can be esterified and dehydrated to produce oxaloacetic acid derivate (the tautomeric isomer of 2-hydroxyfumarate). Secondly, oxaloacetic acid derivate can be hydrogenated via hydrogen transfer process from 1-butanol to form DBMaA. Eventually, DBFA can be produced via dehydration of DBMaA.

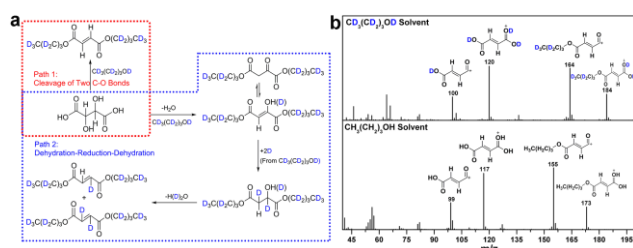


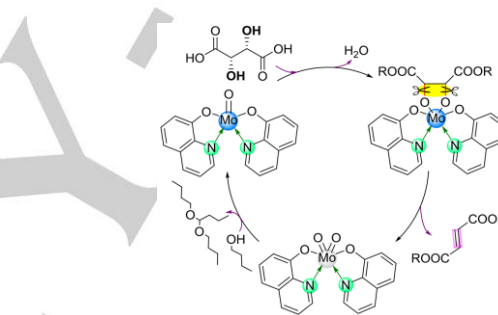
Figure 4. (a) Two proposed pathways of forming DBFA. (b) Mass spectrums of DBFA production in deuterium 1-butanol (up) and 1-butanol (down), respectively.

To determine the formation pathway of DBFA for Mo-8-HQ catalyst, we designed a series of isotopic experiments. For path 1 with concerted mechanism, the H atoms of C=C in DBFA product will keep its intrinsic. For path 2 with stepwise process, more than half of hydrogens on C=C bond in DBFA will come from the environmental hydrogen donor (as shown in Figure 4a). Above all, dimethyl fumarate (DMFA) was added into CD₃OD, and the mixture was treated at 160 °C for 12 h. After reaction, the deuterium content of DMFA was determined by MS. The MS data showed that the molecular weight of deuterium DMFA was $m/z=150$, in contrast to DMFA of $m/z=144$. This result revealed the H atoms on C=C of DMFA were stable under reaction condition (Figure S9). Then, we used deuterium 1-butanol (CD₃(CD₂)₃OD, 1-butanol with all hydrogen deuterated) as the solvent and the reductant, tartaric acid as the substrate and Mo-8-HQ as the catalyst at 160 °C for 12h. The mass spectrums of the products were shown in Figure 4b. Through analyzing significant fragment ions peaks in DBFA product after reacted in deuterium 1-butanol and 1-butanol ($m/z=184$ and 173 , $m/z=164$ and 155 , $m/z=120$ and 117 , $m/z=100$ and 99), all the H atoms located at the C=C bond were not replaced by deuterium atoms from environment. Therefore, we believed that the OH groups were eliminated through concerted cleavage of two C-O bonds (path 1) instead of path 2.

To confirm our inference, intermediate products formed through path 2, including oxaloacetic acid and malic acid, were used as the substrates under the reaction condition with Mo-8-HQ catalyst. Determined by GC, the product was just butyl 2,2-dibutoxypropanoate from the oxaloacetic acid substrate, which possibly resulted from the decarboxylation process of oxaloacetic acid, and the complete conversion of malic acid was almost produced DBMaA (Figure S10). The similar result was obtained when MoO₂(acac)₂ catalyst was used (Figure S11). The absence

of main product DBFA in these experiments indicated that oxaloacetic acid and malic acid were not intermediate products of forming DBFA pathway. It was also corroborated that DBFA cannot be produced from path 2, it should be produced in one-step by path 1. We used a series of experiments to confirm the DBFA formation process, and it was very important for understanding the real mechanism of Mo-catalyzed didehydroxylation reactions of polyhydroxy compounds.

Therefore, the possible mechanism of the whole reaction cycle was proposed in Scheme 2. Single-site Mo^{VI} catalyst was firstly reduced to Mo^{IV} by 1-butanol. Subsequently, Mo^{IV} was condensed with two hydroxyl groups in tartaric acid through a five-membered ring to form a Mo-diolate intermediate. Then, the olefin was extruded from Mo^{IV} catalysts via concerted cleavage of two C-O bonds accompanying with reforming Mo^{VI}, which has been reported as a rate-limiting step. Aforementioned, the single Mo center was in the rich electron condition after coordinating with strong 8-HQ ligands, this will facilitate Mo^{IV} losing two electrons and turning back to Mo^{VI}. In this regard, it also accelerated the extrusion of olefin simultaneously, leading to conquer the rate-limiting transition state.



Scheme 2. Proposed mechanism of didehydroxylation process catalyzed by Mo-8-HQ.

In summary, Mo-8-HQ catalyst with single molybdenum sites was synthesized by ligand exchange method. It exhibits high-efficiency performance for didehydroxylation of biomass-derived dibutyl tartrate, and the high yield of dibutyl fumarate product reached up to 86% at 160 °C. After the reaction, the catalyst could be separated by filtration. Moreover, the pathway of didehydroxylation reaction through concerted cleavage of two C-O bonds was demonstrated via original experimental observation in our deuterium isotopic studies. It was suggested that the excellent catalytic performance of Mo-8-HQ for didehydroxylation reactions might be attributed to the stabilized single Mo sites with electron-rich Mo centers. The results we presented herein demonstrated a specific direction to design economic Mo-based catalysts for didehydroxylation reactions of polyhydroxy compounds. We believe that our work exploits new opportunities for using abundant molybdenum catalysts in industrial applications.

Acknowledgements

This work was financially supported by the National Natural Science Foundation of China (No. 21872139 and 21790331), the

COMMUNICATION

National Key R&D Program of China (2018YFB1501601), the Strategic Priority Research Program of the Chinese Academy of Sciences (XDB17020300), and Dalian Science Foundation for Distinguished Young Scholars (No. 2016RJO8) for scientific research.

Conflict of interest

The authors declare no conflict of interest.

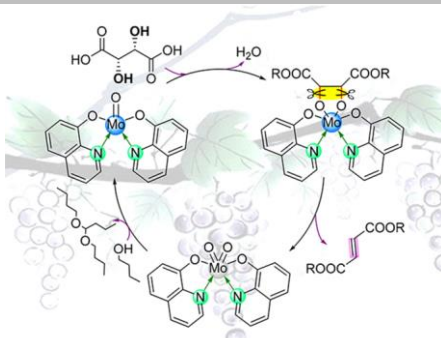
Keywords: biomass • dicarboxylic acid monomer • single-site molybdenum • didehydroxylation • cleavage of C-O bonds

- [1] a) G. W. Huber, J. N. Chheda, C. J. Barrett, J. A. Dumesic, *Science* **2005**, 308, 1446-1450; b) M. S. Holm, S. Saravanamurugan, E. Taarning, *Science* **2010**, 328, 602-605; c) H. Li, S. Saravanamurugan, S. Yang, A. Riisager, *Green Chem.* **2016**, 18, 726-734; d) W. Deng, Y. Wang, S. Zhang, K. M. Gupta, M. J. Hülsley, H. Asakura, L. Liu, Y. Han, E. M. Karp, G. T. Beckham, P. J. Dyson, J. Jiang, T. Tanaka, Y. Wang, N. Yan, *Proc. Natl. Acad. Sci. U. S. A.* **2018**, 115, 5093-5098; e) P. Sudarsanam, R. Zhong, S. Van den Bosch, S. M. Coman, V. I. Parvulescu, B. F. Sels, *Chem. Soc. Rev.* **2018**, 47, 8349-8402.
- [2] X. Wu, X. Fan, S. Xie, J. Lin, J. Cheng, Q. Zhang, L. Chen, Y. Wang, *Nat. Catal.* **2018**, 1, 772-780.
- [3] a) M. Shiramizu, F. D. Toste, *Angew. Chem. Int. Ed.* **2013**, 125, 13143-13147; b) X. Li, Y. Zhang, *ChemSusChem* **2016**, 9, 2774-2778; c) R. Lu, F. Lu, J. Chen, W. Yu, Q. Huang, J. Zhang, J. Xu, *Angew. Chem. Int. Ed.* **2016**, 55, 249-253; d) R. T. Larson, A. Samant, J. Chen, W. Lee, M. A. Bohn, D. M. Ohlmann, S. J. Zuend, F. D. Toste, *J. Am. Chem. Soc.* **2017**, 139, 14001-14004.
- [4] Q. Zhang, J. Chang, T. Wang, Y. Xu, *Energy Convers. Manage.* **2007**, 48, 87-92.
- [5] a) W. Luo, M. Sankar, A. M. Beale, Q. He, C. J. Kiely, P. C. A. Bruijninx, B. M. Weckhuysen, *Nat. Commun.* **2015**, 6, 6540; b) Q. Xia, Z. Chen, Y. Shao, X. Gong, H. Wang, X. Liu, S. F. Parker, X. Han, S. Yang, Y. Wang, *Nat. Commun.* **2016**, 7, 11162.
- [6] A. M. Ruppert, K. Weinberg, R. Palkovits, *Angew. Chem. Int. Ed.* **2012**, 51, 2564-2601.
- [7] L. Yang, G. Tsilomelekis, S. Caratzoulas, D. G. Vlachos, *ChemSusChem* **2015**, 8, 1334-1341.
- [8] a) E. Arceo, J. A. Ellman, R. G. Bergman, *J. Am. Chem. Soc.* **2010**, 132, 11408-11409; b) M. Shiramizu, F. D. Toste, *Angew. Chem. Int. Ed.* **2012**, 124, 8206-8210; c) X. Li, D. Wu, T. Lu, G. Yi, H. Su, Y. Zhang, *Angew. Chem. Int. Ed.* **2014**, 53, 4200-4204.
- [9] A. K. Hijazi, N. Radhakrishnan, K. R. Jain, E. Herdtweck, O. Nuyken, H.-M. Walter, P. Hanefeld, B. Voit, F. E. Kühn, *Angew. Chem. Int. Ed.* **2007**, 46, 7290-7292.
- [10] S. Ishikawa, Y. Maegawa, M. Waki, S. Inagaki, *ACS Catal.* **2018**, 8, 4160-4169.
- [11] M. J. Koh, T. T. Nguyen, J. K. Lam, S. Torker, J. Hyvl, R. R. Schrock, A. H. Hoveyda, *Nature* **2017**, 542, 80-85.
- [12] A. R. Petersen, P. Fristrup, *Chem. Eur. J.* **2017**, 23, 10235-10243.
- [13] a) J. R. Dethlefsen, D. Lupp, B.-C. Oh, P. Fristrup, *ChemSusChem* **2014**, 7, 425-428; b) J. R. Dethlefsen, D. Lupp, A. Teshome, L. B. Nielsen, P. Fristrup, *ACS Catal.* **2015**, 5, 3638-3647; c) S. C. A. Sousa, A. C. Fernandes, *Coord. Chem. Rev.* **2015**, 284, 67-92.
- [14] a) H. Gehrke, J. Veal, *Inorg. Chim. Acta* **1969**, 3, 623-627; b) J. M. Berg, R. H. Holm, *J. Am. Chem. Soc.* **1985**, 107, 917-925; c) M. Stalpaert, D. De Vos, *ACS Sustainable Chem. Eng.* **2018**, 6, 12197-12204.
- [15] A. Syamal, M. R. Maurya, *Coord. Chem. Rev.* **1989**, 95, 183-238
- [16] M. B. Sreedhara, A. L. Santhosha, A. J. Bhattacharyya, C. N. R. Rao, *J. Mater. Chem. A* **2016**, 4, 9466-9471.
- [17] J. J. Concepcion, M.-K. Tsai, J. T. Muckerman, T. J. Meyer, *J. Am. Chem. Soc.* **2010**, 132, 1545-1557.
- [18] a) J. Zhao, L. Xu, *Inorg. Chim. Acta* **2008**, 361, 2385-2395; b) M. Luisa Ramos, L. L. G. Justino, P. E. Abreu, S. M. Fonseca, H. D. Burrows, *Dalton Trans.* **2015**, 44, 19076-19089.
- [19] a) W. A. Herrmann, F. E. Kühn, *Acc. Chem. Res.* **1997**, 30, 169-180; b) C. C. Romão, F. E. Kühn, W. A. Herrmann, *Chem. Rev.* **1997**, 97, 3197-3246; c) S. Raju, M.-E. Moret, R. J. M. Klein Gebbink, *ACS Catal.* **2015**, 5, 281-300.
- [20] R. Lu, F. Lu, X. Si, H. Jiang, Q. Huang, W. Yu, X. Kong, J. Xu, *ChemSusChem* **2018**, 11, 1621-1627.
- [21] a) T. J. Korstanje, E. Folkertsma, M. Lutz, J. T. B. H. Jastrzebski, R. J. M. Klein Gebbink, *Eur. J. Inorg. Chem.* **2013**, 2013, 2195-2204; b) D. B. Larsen, A. R. Petersen, J. R. Dethlefsen, A. Teshome, P. Fristrup, *Chem. Eur. J.* **2016**, 22, 16621-16631.

COMMUNICATION

COMMUNICATION

Directing the selectivity in single-site molybdenum catalyzed synthesis of fumarate via enhancing the concerted cleavage of two C-O bonds pathway



Huifang Jiang, Rui Lu, Xiaoqin Si,
Xiaolin Luo, Jie Xu, and Fang Lu*

Page No. – Page No.

Single-Site Molybdenum Catalyst
for the Synthesis of Fumarate